STEM CELLS AND DEVELOPMENT
Volume 20, Number 11, 2011

DOI: 10.1089/scd.2010.0437

L3MBTL1 Deficiency Directs the Differentiation of Human Embryonic Stem Cells Toward Trophectoderm

Ruben Hoya-Arias,[1] Mark Tomishima,[2] Fabiana Perna,[1] Francesca Voza,[1] and Stephen D. Nimer[1]

Human embryonic stem cells (hESCs) can be used to study the early events in human development and, hopefully, to understand how to differentiate human pluripotent cells for clinical use. To define how L3MBTL1, a chromatin-associated polycomb group protein with transcriptional repressive activities, regulates early events in embryonic cell differentiation, we created hESC lines that constitutively express shRNAs directed against L3MBTL1. The L3MBTL1 knockdown (KD) hESCs maintained normal morphology, proliferation, cell cycle kinetics, cell surface markers, and karyotype after 40 passages. However, under conditions that promote spontaneous differentiation, the L3MBTL1 KD cells differentiated into a relatively homogeneous population of large, flat trophoblast-like cells, unlike the multilineage differentiation seen with the control cells. The differentiated L3MBTL1 KD cells expressed numerous trophoblast markers and secreted placental hormones. Although the L3MBTL1 KD cells could be induced to differentiate into various embryonic lineages, they adopted an exclusive trophoblast fate during spontaneous differentiation. Our data demonstrate that depletion of L3MBTL1 does not affect hESC self-renewal, rather it enhances differentiation toward extra-embryonic trophoblast tissues.

Introduction

Human embryonic stem cells (hESCs) are derived from the inner cell mass of early preimplantation blastocysts; they self-renew and are pluripotent. They can be maintained in an undifferentiated state, but can also be induced to differentiate into cell types characteristic of all 3 germ layers and of extra-embryonic tissues, offering the potential to model aspects of mammalian development and disease. Indeed, progress made over the past decade has determined that directing hESCs toward specific cell fates requires similar kinetics and signaling pathways as those required during development [1].

The trophoblast is an essential extra-embryonic tissue that arises from pluripotent trophectoderm (TE) during mammalian development. Interplay between transcriptional, epigenetic, and physiological factors governs TE cell fate. Several transcription factors including Cdx2, Tead4, Eomes, Gata3, Elf5, Ets2, and Tcfap2c are involved in TE lineage specification and its further expansion [2–8]. Differential epigenetic modifications including DNA methylation [9] and the distribution of histone modifications and their modifying enzymatic complexes [10–13] contribute to lineage identity in the early embryo by regulating the appropriate gene expression profiles. Because in vitro cell fate decisions are similar to those made during development in vivo, hESCs can be exploited to reveal critical aspects of human development.

The *Drosophila* lethal 3 malignant brain tumor protein, D-l(3)mbt, functions as a tumor suppressor in the larval brain [14]. The gene encoding its human homolog, L3MBTL1, is located on chromosome 20q12, within a region commonly deleted in myeloid malignancies [15], suggesting that it may also function as a tumor suppressor in mammals. L3MBTL1 functions as a transcriptional repressor [16] and chromatin compactor [17]; in vitro biochemical studies have shown that the L3MBTL1 MBT domains can compact nucleosomal arrays dependent on the mono- or dimethylation of histone H4K20 and H1bK26 [17,18]. We have recently demonstrated that L3MBTL1 depletion enhances the differentiation of hematopoietic stem cells toward the erythroid lineage [19], and its depletion from differentiated, malignant cell lines causes replicative stress, DNA breaks, activation of the DNA damage response, and genomic instability [20].

We hypothesized that as a chromatin-associated protein with repressor properties, changes in the level of L3MBTL1 activity could alter the chromatin structure and influence the ability of hESCs to either self-renew or commit to differentiation. To test this hypothesis, we generated and characterized 2 independent and stable clones of L3MBTL1-depleted hESCs, using a lentiviral vector system to express short hairpin RNAs (shRNAs) directed against L3MBTL1 mRNA.

[1]Molecular Pharmacology and Chemistry Program and [2]SKI Stem Cell Research Facility, Sloan-Kettering Institute, Memorial Sloan-Kettering Cancer Center, New York, New York.

Although the self-renewal properties of L3MBTL1 knockdown (KD) hESCs were retained, we observed striking morphological changes when L3MBTL1 KD hESCs spontaneously differentiated and established that they spontaneously differentiate into trophoblast-like cells. L3MBTL1 appears to be an important regulator of early cell fate decisions during mammalian development.

Materials and Methods

shRNA design and cloning

The design and cloning of shRNAs into the H1P-Hygro/EGFP lentiviral plasmid was done essentially as previously described [21]. RNA sequences were selected using the Dharmacon SMARTselection design software. Forward and reverse oligonucleotides were resuspended at a concentration of 5 μM, heated to 95°C for 5 min, and allowed to cool to RT overnight. After annealing, the duplexes were cloned into *Sma*I/*Xba*I sites of an H1P shRNA cassette. The sequences targeted by the shRNAs are as follows: L3MBTL1 shRNA1: 5′-GTAGTGAGTTGTAGATAAA-3′; L3MBTL1 shRNA2: 5′-GTGGAATCATTGACAGAAA-3′; luciferase control shRNA: 5′-CCCGGAAAGACGATGACGG-3′.

Cell culture and differentiation protocols

hESC line H9 (WA-09) cells were cultured on a feeder layer of mouse embryonic fibroblast (MEFs), purchased from GlobalStem, and plated on gelatin-coated tissue culture plates. ES cells were maintained in an undifferentiated state in human ES (HES) media (DMEM:F12; Invitrogen) supplemented with 20% knockdown serum replacement (Invitrogen), 1% nonessential amino acids (Invitrogen), 0.1 mmol/L 2-mercaptoethanol (Invitrogen), 1 mmol/L L-glutamine (Invitrogen), and 6 ng/mL FGF2 (R&D Systems). Cells were passaged using Dispase (neural protease; Worthington Bioscience).

Spontaneous differentiation was induced by plating control and L3MBTL1KD cells in feeder-free conditions on Matrigel (BD Bioscience)-coated dishes in HES medium without FGF2 for 2 weeks; cells were fed daily. The day on which the cells were seeded was defined as day 1.

Embryoid bodies (EBs) were generated by culturing control and L3MBTL1 KD cells in low-cell-binding dishes for 14 days with the same medium used in spontaneous differentiation. EBs were collected by gravity and fed every other day.

The directed differentiation to trophoblast was achieved by culturing the cells on Matrigel-coated dishes in HES medium in the presence of exogenous BMP4 (100 ng/mL), as previously described [22]. Differentiation toward neuroectoderm was performed using a published protocol [23]. Briefly, control and L3MBTL1 KD cells were cocultured on MS-5 stroma cells and fed with KSR medium supplemented with SB431542 (10 μM/mL) and dorsomorphin (600 nM/mL) during the first 7 days; then cells were fed only with KSR medium until day 14.

Production of stable L3MBTL1-deficient embryonic stem cell lines

The H1P-HygroEGFP plasmid expressing shRNA against L3MBTL1 was cotransfected with plasmids pMD2.G and psPAX2 into 293T cells to make lentiviral particles. Virus-containing media was collected, filtered, and concentrated by ultracentrifugation. Viral titers were measured by serial dilution on 293T cells followed by flow cytometry analysis after 48 h. For transduction, lentiviral vectors were added to H9 cells maintained without feeders on Matrigel-coated plates. To select clones, colonies were treated with Accutase (Innovative CT/ISC Bioexpress) for 30 min at 37°C, leaving a single-cell suspension. The Accutase was neutralized with 3 volumes of HES medium and the cells were resuspended by pipetting before being filtered using a 70-μm nylon filter (Falcon, BD Bioscience). The cells were centrifuged and washed 2× with HES media and then 2× in ice-cold PBS with 1% BSA. The pelleted cells were resuspended in 100 μL ice-cold PBS with 1% BSA supplemented with 10 μM Y27632 (ROCK inhibitor purchased from Calbiochem). GFP-positive cells were sorted using a BD FACSAria cell sorter (BD Bioscience) and resuspended in HES media with 10 μM Y27632 and penicillin/streptomycin 1,000 U/mL and replated on MEF feeders. Y27632 and penicillin/streptomycin were maintained in the medium until the first colonies appeared. Several clones for each shRNA construct were selected and quantitative polymerase chain reaction (qPCR) analysis was performed to ascertain viral copy number and the efficiency of L3MBTL1 knockdown.

Reverse transcriptase and real time polymerase chain reaction

Total RNA was isolated from undifferentiated and differentiated hESCs growing as monolayers using the RNeasy® Plus Kit (Qiagen). cDNA was synthesized from 1 μg total RNA using Moloney murine leukemia virus RT (Promega) in 1× transcription buffer containing 0.5 μmol/L oligo dT (Promega) and 400 μmol/L deoxyribonucleotides (dNTPs). Reverse transcriptase (RT) qPCR was performed with the ABI 7500 real-time PCR system with SYBR green (ABI) and 200 nM of forward and reverse primers. A standard curve was generated for each primer pair, and genes of interest were assigned a relative expression value interpolated from the standard curve using the threshold cycle (Ct). Gene expression was normalized against the level of GAPDH expression. All reactions were done in duplicate, and at least 4 technical and 2 biological replicates were performed. PCR primer sequences are shown in Table 1 and Supplementary Table S1.

Immunofluorescence

Cultured cells were washed twice with PBS before being fixed in 4% paraformaldehyde at room temperature. Cells were washed 3 times with PBS before permeabilization with wash buffer (0.3% Triton X-100 and 1.0% bovine serum albumin in PBS) for at least 5 min. The primary antibody (diluted in wash buffer) was added to the cells for 2 h at room temperature, and then the cells were washed 3 times in wash buffer before the addition of the secondary antibody (diluted in wash buffer) for 1 h at room temperature. The cells were washed 3 times with PBS and stored at 4°C. The primary antibodies OCT-3/4 (4 μg/mL; sc-5279), HAND1 (0.4 μg/mL; Ab11846), and L3MBTL1 (1:50 dilution) previously described [16] were detected using the appropriate secondary

Table 1. List of Oligonucleotides Used in Reverse Transcriptase qPCR

Gene	*Forward*	*Reverse*
L3MBTL1	AGAGGAAGCGCAGGGAATA	CACGACCAGCATTCCTTCTT
OCT4	CCTCCAGCAGATGCAAGAA	ATTGGAAGGTTCCCAGTCG
NANOG	CCTCCAGCAGATGCAAGAA	ATTGGAAGGTTCCCAGTCG
CDX2	GTCTTTTTTCTCTTCCCTTCCC	CAACAACACAAACTCCCCC
SOX2	ACCAGCGCATGGACAGTTA	ATGTAGGTCTGCGAGCTG GT
AFP	CTTCCAAACAAAGGCAGCA	ATGTACATGGGCCACATCC
SOX1	ATGCACCGCTACGACATGG	CTCATGTAGCCCTGCGAGTTG
ACTC1	CCCTGGAGAAGAGCTATGAAC	GGAAGGTAGATGGAGAGAGAA G
CGB	GTGGAGAAGGAGGGCTGC	GGCGGCAGAGTGCACATT
HAND1	TGCCTGAGAAAGAGAACCAG	ATGGCAGGATGAACAAACAC
KRT 7	TGAATGATGAGATCAACTTCCTCAG	GCAGTCCCAGATCTCCGACA
KRT 8	GATCGCCACCTACAGGAAGCT	ACTCATGTTCTGCATCCCAGACT
GCM1	GAGCCTGGAGACCGAGAAC	TTGCGAAGATCTGAGCCC
PAX6	CGGAGTGAATCAGCTCGGTG	CCGCTTATACTGGGCTATTTTGC
GAPDH	GGTCGGAGTCAACGGATTT	GCCCCACTTGATTTTGGAG

l3mbtl1, l(3)mbt-like 1 (*Drosophila*); OCT4, POU class 5 homeobox 1; NANOG, nanog homeobox; CDX2, caudal type homeobox 2; SOX2, SRY (sex-determining region Y)-box 2; AFP, alpha-fetoprotein; SOX1, SRY (sex-determining region Y)-box 1; ACTC1actin, alpha, cardiac muscle 1; GCB, chorionic gonadotropin, beta polypeptide; HAND1, heart and neural crest derivatives expressed 1; KRT7/8, keratin 7/8; GCM1, glial cells missing homolog 1; PAX6, paired box 6; GAPDH, glyceraldehyde-3-phosphate dehydrogenase.

antibodies conjugated with Alexa Fluor 546 (Molecular Probes). Negative controls consisted of no primary antibody, no secondary antibody, or the appropriate IgG isotype control as indicated. DAPI counterstaining was performed on fixed cells to visualize all cellular nuclei.

Western blot analysis

Total cellular protein extracts were prepared using RIPA buffer (SIGMA R0278) supplemented with Halt Protease Inhibitor Cocktail (Thermo Scientific 78430) according to the manufacturer's instructions. Nuclear and cytoplasmic extracts were prepared using the PIERCE kit (78833) for subcellular fractionation; 40 μg of protein extracts were electrophoresed on a 4–12% denaturing gel and electroblotted onto a nitrocellulose membrane. The membrane was incubated with different antibodies at 4°C overnight and then incubated with the indicated secondary antibodies at room temperature for 1 h. The Pierce Enhanced Chemiluminescence kit was used to detect antibody reactivity, according to the manufacturer's instructions.

Cell cycle/DNA and flow cytometry analysis

To analyze DNA content, control and L3MBTL1 KD ES cells were cultured on Matrigel-coated tissue culture-treated dishes, harvested by trypsinization, washed with PBS, and fixed in 70% EtOH at 4°C. The cells were washed with PBS, resuspended in propidium iodide solution (5 μg/mL) containing 10 mg/mL RNase, mixed, and incubated 45 min at 37°C. Flow cytometric data were acquired on a BD FACSCalibur (BD Biosciences) using CellQuest Pro version 6.0. Propidium iodide was excited by the 488 nm laser and fluorescence emission was measured in fluorescence parameter 3 (FL3) with the standard 670LP filter. Doublets were excluded by gating out high FL3-W (width) cells. Single cells were analyzed for percentages of G1/G0, S, and G2/M in MultiCycle AV (Innovative Cell Technologies).

Detection of trophoblast marker HLA-G in L3MBTL1 KD spontaneously differentiated cells was performed by immunostaining with an APC-labeled anti-human HLA-G (eBioscience 17-9957 clone 87G) using 0.125 μg/sample; 7-AAD (5 μg/mL) staining served to exclude dead cells from subsequent analysis. For each sample, 5×10^4 cells were analyzed on a FACS Calibur flow cytometer (BD Biosciences) using CELLQuest (BD Biosciences); data analysis was performed using the FlowJo software (Tree Stars, Inc.).

Immunoassays

Media were collected from growing cells and stored at −20°C until assay. Chorionic gonadotropin (CG-β) and progesterone levels were measured using ELISA kits, as indicated by the manufacturer (Calbiotech).

Statistical analysis

Data were analyzed using PRISM Version 5.04 (GraphPad Software, Inc.). Sample comparison was performed using 1-way analysis of variance (ANOVA) followed by a post-hoc Tukey test or 2-way ANOVA followed by a post-hoc Bonferroni test, with the level of significance set at $P < 0.05$.

Results

L3MBTL1 knockdown does not affect embryonic stem cell renewal

We initially screened 10 different shRNAs that target L3MBTL1 using K562 cells (data not shown) and used the 4 most efficient shRNAs to transduce H9 hESCs. Ultimately, 2 shRNAs were used (shRNA1 and shRNA2) (Fig. 1A) that most consistently knocked down L3MBTL1 in H9 cells compared with the H9 cells expressing a nontargeting, luciferase-specific hairpin (LUC shRNA) and the parental H9 cell line. Overall, 11 L3MBTL1 KD ES cell clones were generated. Western blot (Fig. 1B) and immunofluorescence analysis (Supplementary Fig. S1; Supplementary Data are

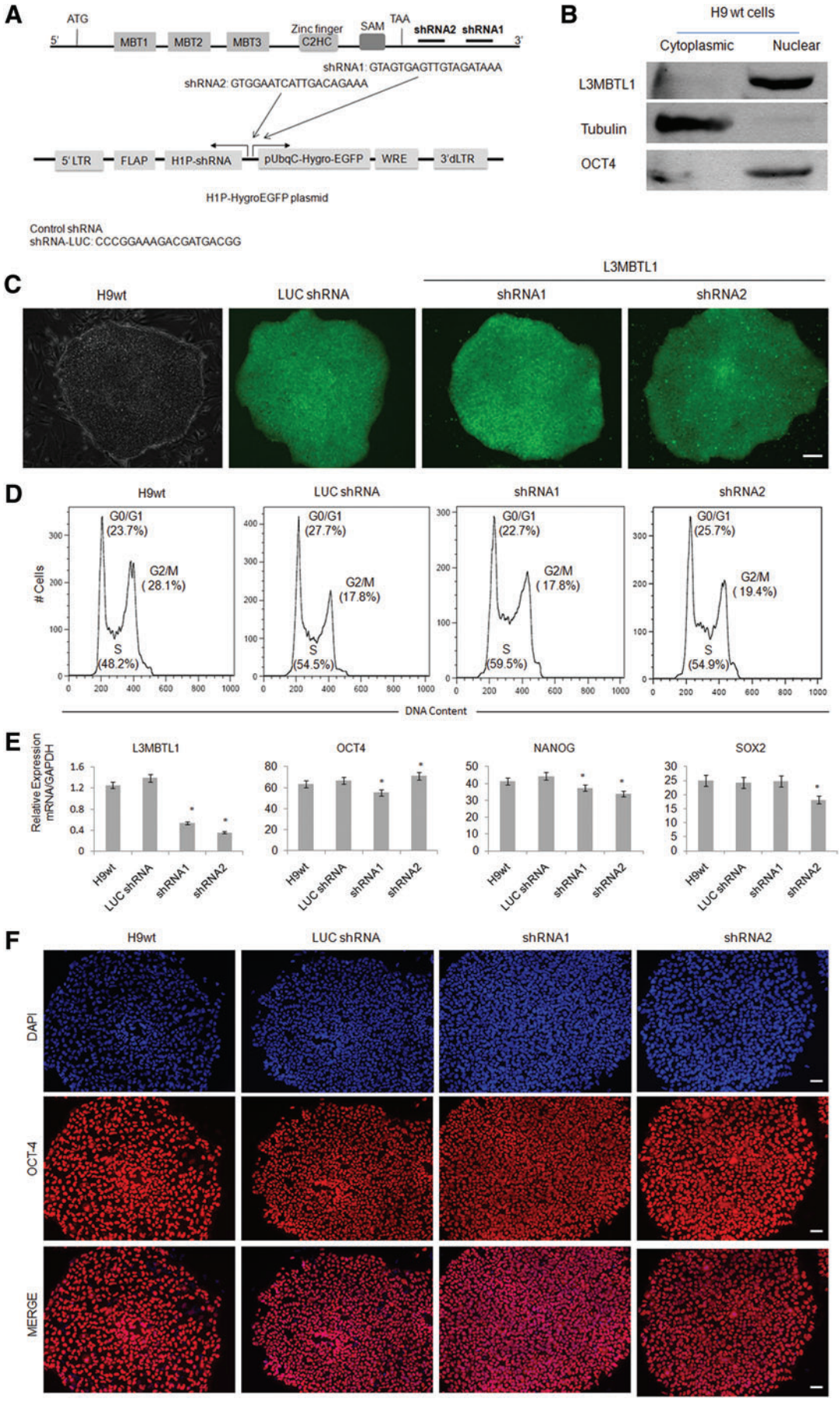
A
ATG
5'
MBT1
MBT2
MBT3
Zinc finger C2HC
SAM
TAA
shRNA2 shRNA1
3'
shRNA1: GTAGTGAGTTGTAGATAAA
shRNA2: GTGGAATCATTGACAGAAA
5' LTR
FLAP
H1P-shRNA
pUbqC-Hygro-EGFP
WRE
3'dLTR
H1P-HygroEGFP plasmid
Control shRNA
shRNA-LUC: CCCGGAAAGACGATGACGG
B
H9 wt cells
Cytoplasmic
Nuclear
L3MBTL1
Tubulin
OCT4
C
L3MBTL1
H9wt
LUC shRNA
shRNA1
shRNA2
D
H9wt
LUC shRNA
shRNA1
shRNA2
Cells
G0/G1 (23.7%)
G2/M (28.1%)
S (48.2%)
G0/G1 (27.7%)
G2/M (17.8%)
S (54.5%)
G0/G1 (22.7%)
G2/M (17.8%)
S (59.5%)
G0/G1 (25.7%)
G2/M (19.4%)
S (54.9%)
DNA Content
E
Relative Expression mRNA/GAPDH
L3MBTL1
OCT4
NANOG
SOX2
H9wt
LUC shRNA
shRNA1
shRNA2
F
H9wt
LUC shRNA
shRNA1
shRNA2
DAPI
OCT-4
MERGE

available online at www.liebertonline.com/scd) confirm the nuclear localization of L3MBTL1 in ES cells. The L3MBTL1 KD hESCs showed normal colony morphology (Fig. 1C), normal cell cycle kinetics (Fig. 1D), an unchanged pattern of cell surface markers, and a normal karyotype in prolonged culture (data not shown) when cultured under normal hESC growth conditions. We obtained an ~70% reduction in L3MBTL1 mRNA levels (using either shRNA1 or shRNA2) and observed a small decrease in the levels of the pluripotency-promoting OCT-4, NANOG, and SOX2 transcription factor mRNAs (Fig. 1E). Immunofluorescence analysis confirmed the normal expression and localization of OCT-4 protein in all cell lines (Fig. 1F). Thus, L3MBTL1 depletion does not detectably affect the undifferentiated state of hESCs.

L3MBTL1 knockdown impairs embryonic cell production during spontaneous differentiation

To determine whether loss of L3MBTL1 affects differentiation, we withdrew FGF2 from HES media and grew the hESCs under either adherent or nonadherent conditions, inducing their spontaneous differentiation. hESCs were maintained for 2 weeks under adherent culture conditions as colonies, using Matrigel-coated dishes. Depletion of L3MBTL1 had clear morphological consequences, as all 11 clones derived from the shRNA1- or shRNA2-expressing hESCs generated differentiated colonies composed of large, flat mononucleated cells by days 7–14. In contrast, the control luciferase knockdown H9 cells and the parental line H9 generated mixed colonies composed of many different cell morphologies (Fig. 2A and data not shown). We also observed morphological consequences in the EBs generated from L3MBTL1 KD cells under nonadherent conditions; in contrast to the control cells, the L3MBTL1 KD cells failed to give rise to typical EB structures containing differentiated cell types. Starting at day 5 of differentiation, the L3MBTL1 KD EBs underwent significant cell death that continued until day 14, indicating defects in differentiation, whereas control cells developed into characteristic EB structures (Fig. 2B). Flow cytometric analysis for Annexin V binding and 7-AAD permeability confirmed an increased cell death in the L3MBTL1 KD cells compared with the control cells at day 7 of differentiation (Fig. 2C).

To characterize the differentiation state of the L3MBTL1 KD cells in monolayer cultures, we performed reverse transcriptase qPCR analysis to quantify the expression of a variety of pluripotent and lineage-specific markers. Differentiated control and L3MBTL1 KD cells were evaluated and significant differences were seen. As expected, the pluripotency markers OCT-4 and NANOG were reduced in both the L3MBTL1 KD and the control KD cells compared with the undifferentiated cells (Fig. 2D). Of note, L3MBTL1 levels were upregulated at least 3-fold in the differentiated controls compared with the undifferentiated controls, suggesting a potential role for L3MBTL1 in the earliest stages of differentiation. However, the shRNA constructs continued to suppress L3MBTL1 mRNA levels despite the increased expression that have occurred during normal differentiation (Fig. 2D). Quantification of lineage marker expression shows downregulation of the SOX1 (ectoderm) and AFP (endoderm) markers in the L3MBTL1 KD cells, compared with their increased levels in the differentiated controls. Interestingly, we observed a substantial upregulation in the expression of ACTC1 (mesoderm) and the trophoblast marker chorionic gonadotropin (CG-β) in the L3MBTL1 KD in contrast to the differentiated control cells (Fig. 2E). We also performed reverse transcriptase qPCR analysis to assess the expression of additional lineage markers including NEUROD1, SOX2, MAP2 (ectoderm); HNFA4, FOXA2, PECAM1 (endoderm); and MIXL1, RUNX1, and RUNX2 (mesoderm). These studies confirmed that ectoderm, endoderm, and mesoderm derivatives are severely reduced, and of the mesodermal markers, only RUNX1 was upregulated in the L3MBTL1 KD cells (3-fold) compared with the differentiated control cells (Supplementary Fig. S2). Consistent with this finding, RUNX1 has been reported to be an L3MBTL1 target gene in K562 cells [24]. These results show that L3MBTL1 KD cells have a bias to differentiate into trophectoderm following FGF2 withdrawal, whereas ectoderm and endoderm differentiation appears to be blocked.

L3MBTL1 knockdown promotes differentiation of hESCs toward trophectoderm

The flat cell morphology (Fig. 2A) and the greater than 18-fold upregulation of CG-β in the differentiated L3MBTL1 KD cells (Fig. 2E) led us to examine the expression of other trophoblast markers, including CDX2 [25–27], HAND1 [28–31], KRT7, KRT8, and GCM1 [22,27,31–34]. CDX2 mRNA upregulation parallels the appearance of morphological changes in spontaneously differentiated L3MBTL1 KD cells by days 6–7, reaching a peak on day 9; in contrast, HAND1, KRT7, KRT8, and GCM1 mRNAs peak at day 14. The expression pattern of these markers further indicates that L3MBTL1 KD cells primarily differentiate into trophoblast cells (Fig. 3A, B). We have confirmed that HAND1 protein is

FIG. 1. Characterization of undifferentiated control and L3MBTL1 knockdown (KD) human embryonic stem cells. **(A)** Schematic representation of L3MBTL1 gene showing the location for the short hairpin (shRNA) sequences cloned into the H1P-HygroEGFP lentiviral plasmid. **(B)** Western blot of cytoplasmic and nuclear fractions from H9 parental cells shows nuclear location of L3MBTL1. Oct4 (nuclear) and tubulin (cytoplasmic) were used as controls. **(C)** Microscopic images showing the undifferentiated stage for the wt parental, LUC shRNA, L3MBTL1-shRNA1, and shRNA2 H9 cells based on their expression of GFP. Whole colonies were imaged on an Olympus epifluorescence system under a 10× objective. Scale bar represents 100 μm. **(D)** Cell cycle analysis of undifferentiated control and L3MBTL1KD ES cells. Relative DNA content, assessed by PI staining, shows the proportion of cells in the G1, G2, and S phases. A representative example of 3 independent experiments is shown. **(E)** Reverse transcriptase qPCR analysis comparing the level of L3MBTL1, OCT-4, NANOG, and SOX2 mRNA expression in control and L3MBTL1-depleted cells. Statistical analysis was performed by 1-way ANOVA and Tukey posttest (*$P < 0.05$). Error bars represent the standard deviation ($n = 3$). **(F)** Fluorescent microscopy images of OCT-4 with a DAPI DNA counterstain using the Olympus epifluorescence system under a 20× objective. Scale bar represents 50 μm. Color images available online at www.liebertonline.com/scd

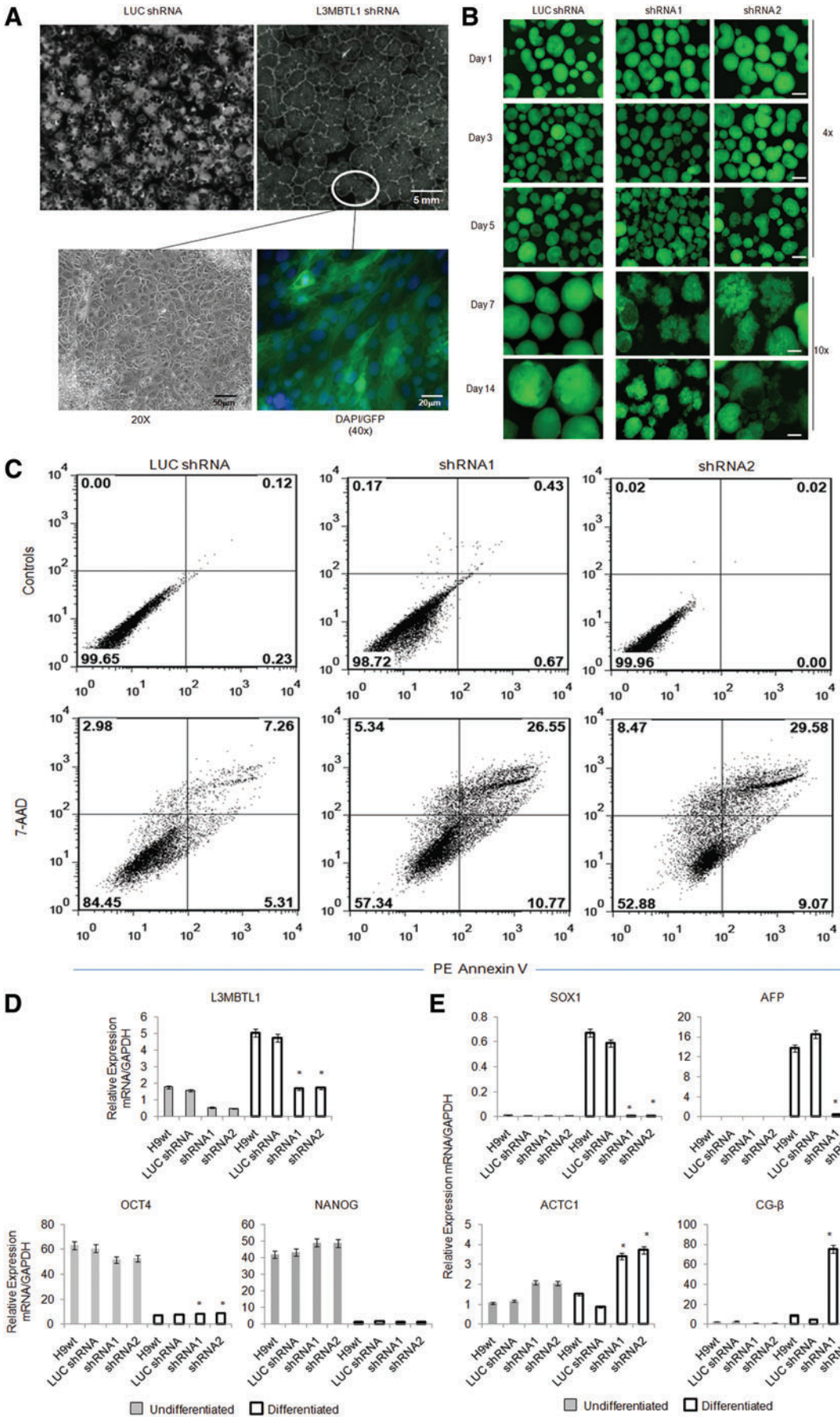
A
LUC shRNA
L3MBTL1 shRNA
5 mm
50μm
20μm
20X
DAPI/GFP
(40x)
B
LUC shRNA
shRNA1
shRNA2
Day 1
Day 3
Day 5
Day 7
Day 14
4x
10x
C
LUC shRNA
shRNA1
shRNA2
Controls
7-AAD
0.00
0.12
99.65
0.23
0.17
0.43
98.72
0.67
0.02
0.02
99.96
0.00
2.98
7.26
84.45
5.31
5.34
26.55
57.34
10.77
8.47
29.58
52.88
9.07
PE Annexin V
D
L3MBTL1
Relative Expression mRNA/GAPDH
OCT4
NANOG
H9wt
LUC shRNA
shRNA1
shRNA2
Undifferentiated
Differentiated
E
SOX1
AFP
ACTC1
CG-β
Relative Expression mRNA/GAPDH
Undifferentiated
Differentiated

expressed in differentiated L3MBTL1 KD cells by immunofluorescence (Fig. 3C) and that more than 80% of the cells analyzed at day 14 of differentiation have trophectoderm phenotype, as indicated by the expression of HLA-G (Fig. 3D).

To further examine the differentiation of L3MBTL1 KD cells into trophoblasts, we directed control cells toward trophoblasts using BMP4 [22]. We compared the gene expression pattern of the BMP4-treated control (LUC shRNA) cells with the spontaneously differentiated L3MBTL1 KD cells and found similar but higher trophoblast marker expression (CG-β and HAND1) in the BMP4-treated control cells (Fig. 4A). Of note, L3MBTL1 expression decreased at least 4-fold in the control cells treated with BMP4 compared with untreated LUC shRNA control, which is also consistent with the notion that downregulation of L3MBTL1 allows trophoblast formation to proceed in hESCs (Figs. 2D and 4A). To further investigate the role of BMP signaling, we measured the level of phosphorylated SMAD proteins (SMAD 1/5/8) during the spontaneous differentiation of the LUC shRNA and L3MBTL1 KD cells. We found an increased level of phospho-SMAD 1/5/8 in differentiated L3MBTL1 KD cells compared with the control cells (Fig. 4B). We also measured the secretion of the placental hormones CG-β and progesterone into the medium from spontaneously differentiated L3MBTL1 KD cells and also the untreated and BMP4-treated controls. L3MBTL1 KD and BMP4-treated control cells show a continuous increase in the concentration of both hormones, with the hormone secretion by the knockdown cells being nearly as high as from the BMP-treated control (Fig. 4C). These results show that L3MBTL1 KD cells differentiate into functional trophoblast cells, which indicates the role of L3MBTL1 in regulating the spontaneous differentiation of embryonic derivatives.

Directed differentiation is not impaired in L3MBTL1 KD cells

L3MBTL1 KD cells did not express ectoderm markers under conditions that allow spontaneous differentiation (Fig. 2D). However, to determine whether directed differentiation was affected in L3MBTL1 KD cells, we induced neural differentiation by coculturing them on MS-5 stromal cells for 2 weeks according to an established protocol [23]. We observed neuronal rosette formation on day 8 with all clones (Fig. 4D, upper panel), demonstrating that L3MBTL1 KD cells can differentiate into neuroectoderm if provided with a sufficiently strong signal. Further, reverse transcriptase qPCR analysis found a similar level of induction of the neuroectodermal markers SOX1 and PAX6 in the knockdown versus the control cell lines (Fig. 4D, lower panel). We also directed the differentiation of L3MBTL1 KD hESC toward hematoendothelial cells ($CD31^+CD34^+$) using a previously reported protocol [35] and found that the KD cells responded to these differentiation signals as well, albeit less efficiently than to the controls (data not shown). These results indicate that L3MBTL1 KD does not impair hESC differentiation toward embryonic neuroectoderm or hematoendothelial cells when potent differentiation-promoting signals are provided.

Discussion

Undifferentiated ES cells generally contain more permissive chromatin with higher levels of activating marks (lysine acetylation) and lower levels of repressive marks (H3 lysine K9 and K27 methylation), whereas differentiated ES cells generally display silenced chromatin structure [36]. One of the great challenges in human stem cell biology is to understand the mechanisms that selectively silence certain gene-rich regions of the genome, to allow the production of the full range of cell types found in the adult. Compacted chromatin is generally found during differentiation, but very little is known about the individual proteins that differentially silence genes and affect the outcome of differentiation.

In this study, we found that knocking down the epigenetic "reader" L3MBTL1 strongly influences the differentiation potential of hESCs toward trophectoderm under conditions wherein spontaneous differentiation occurs, without affecting hESC self-renewal in the undifferentiated state. L3MBTL1 KD hESCs can be cultured continuously with no noticeable changes in their behavior, morphology, or cell cycle status and only minor changes in the RNA levels of the pluripotency markers OCT-4, NANOG, or SOX2 (Fig. 1C–E), which suggests that L3MBTL1 does not play a critical role in maintaining the undifferentiated status or self-renewal potential of hESCs.

Nonetheless, L3MBTL1 KD clearly impaired the developmental potential of hESCs in spontaneous differentiation assays. Withdrawal of FGF2 triggered profound changes in the differentiated L3MBTL1 KD cells under adherent conditions with loss of ectoderm, endoderm, and mesoderm marker expression; this implies that L3MBTL1 KD cells have limited pluripotency. The differentiated L3MBTL1 KD cells

FIG. 2. Morphological changes of spontaneously differentiated control and L3MBTL1 KD cells. **(A)** Photographs showing the morphological contrast between LUC shRNA and L3MBTL KD cells (*left* and *right upper row*, respectively); images were acquired using the Gel Doc System Quantity One software (BioRad). Lower row shows a magnified view of the differentiated L3MBTL1 KD cells (*white circle*); black lines show a phase-contrast image (*left*) and a DAPI/GFP fluorescence image (*right*). **(B)** L3MBTL1 KD cells fail to develop proper embryoid bodies. Fluorescent microscopic images showing EB derivation based on GFP expression for the LUC shRNA, shRNA1, and shRNA2 cell lines. Scale bars: 0.2 mm (4×); 100 μm (10×). Representative images of 3 independent experiments are shown. **(C)** Flow cytometry assay shows increasing cell death for the differentiated L3MBTL1 KD EB cells. Top plots show unstained control and L3MBTL1 KD EB cells and bottom plots show PE-Annexin V versus 7-AAD permeability profiles in the same cells. Apoptotic cells on the plots are Annexin V positive and PI negative (*lower right quadrant*), whereas necrotic cells are Annexin V positive and PI positive (*upper right quadrant*). **(D)** Expression of L3MBTL1, OCT-4, and NANOG in undifferentiated and differentiated state measured as relative level of mRNA/GAPDH. **(E)** mRNA expression levels of lineage cell markers SOX1 (ectoderm), AFP (endoderm), ACTC1 (mesoderm), and CG-β (trophoblast) in undifferentiated and differentiated states measured as relative level of mRNA/GAPDH. Statistical analysis was performed by 1-way ANOVA and Tukey posttest (*$P < 0.05$). Error bars represent the standard deviation ($n = 3$). Color images available online at www.liebertonline.com/scd

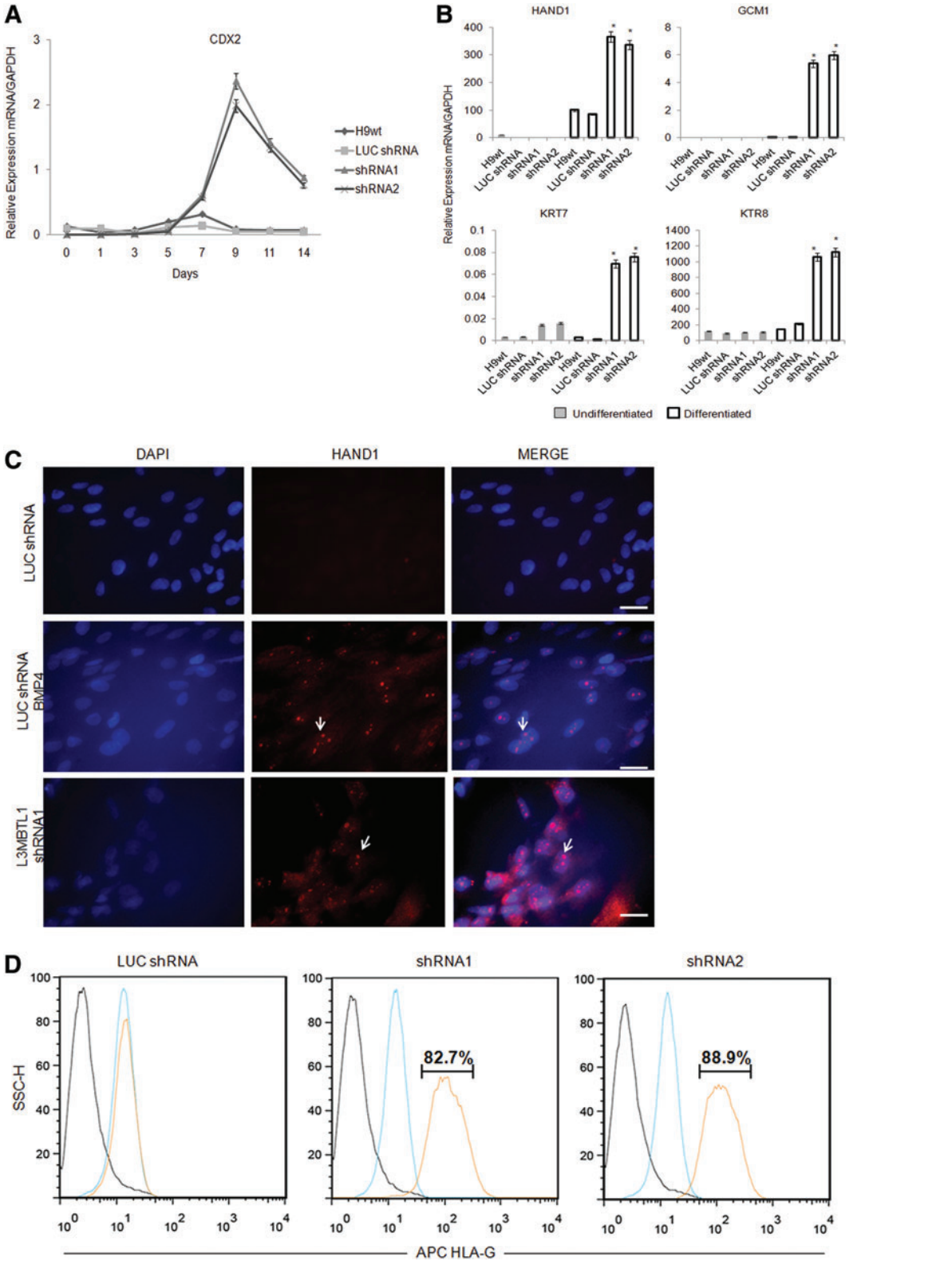

FIG. 3. Reverse transcriptase qPCR analysis for lineage cell markers. **(A)** Relative levels of mRNA expression of trophoblast marker CDX2. Error bars represent the standard deviation ($n=3$). **(B)** Trophoblast cell markers HAND1, GCM1, KRT7, and KRT8 in undifferentiated and differentiated states measured as relative level of mRNA/GAPDH. Statistical analysis was performed by 1-way ANOVA and Tukey posttest ($^*P<0.05$). Error bars represent the standard deviation ($n=3$). **(C)** Immunofluorescent detection of HAND1. *White arrows* indicate the nuclear location of HAND1 protein. Microscopy performed with Olympus epifluorescence system under a 40× objective. Scale bar represents 50 μm. Representative images of 3 independent experiments are shown. **(D)** FACS analysis shows the percentage of spontaneously differentiated control and L3MBTL1 shRNA1 and shRNA2 cells expressing the trophectodermal (TE) marker HLA-G (red). Isotype control antibody staining is shown (black). Undifferentiated LUC shRNA and L3MBTL1 KD cells were used as negative controls for HLA-G staining (blue). Color images available online at www.liebertonline.com/scd

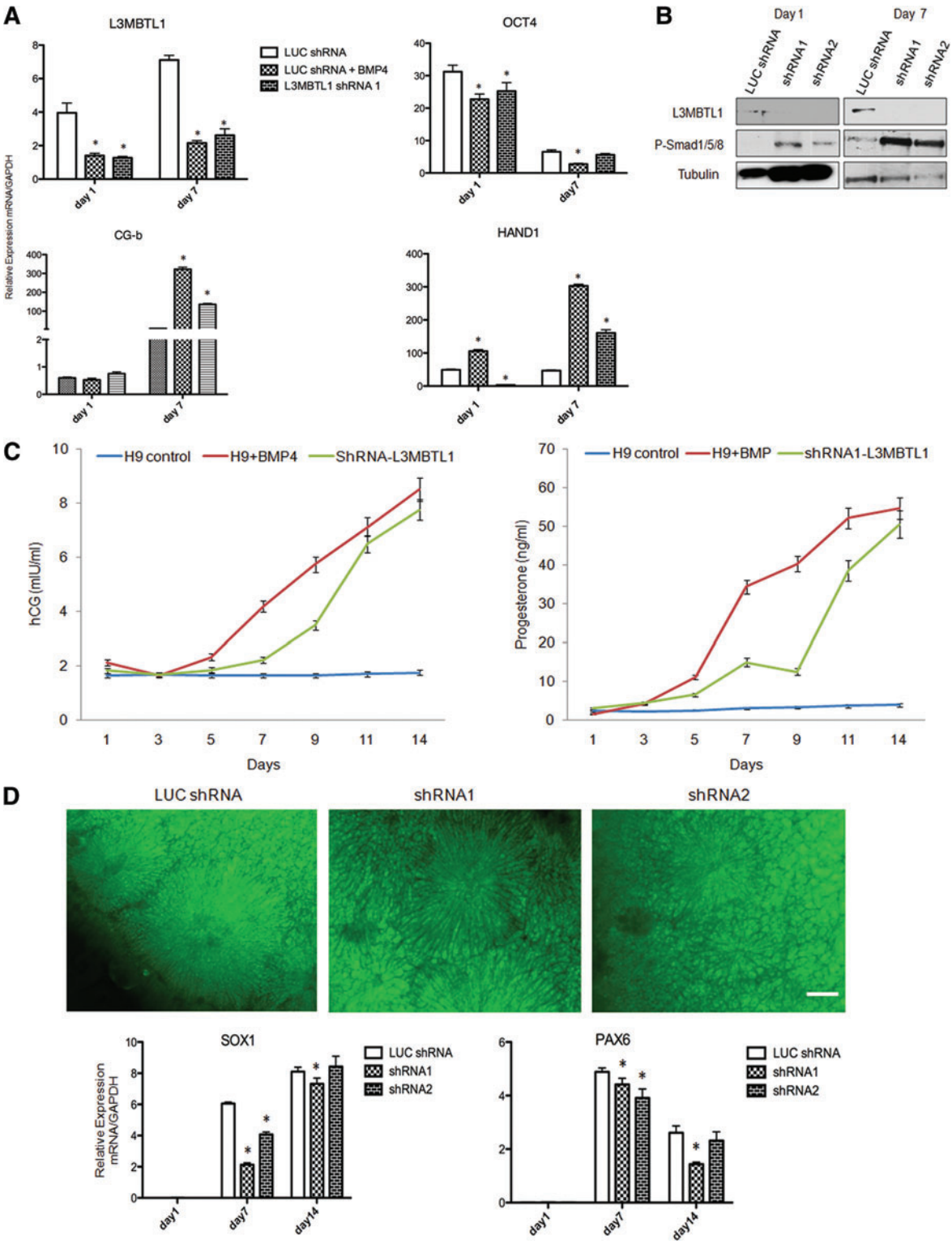

FIG. 4. L3MBTL1 knockdown mimics trophoblast differentiation induced by BMP4. Luciferase control with or without BMP4 and L3MBTL1 KD cells were cultured for 7 days. **(A)** Reverse transcriptase qPCR analysis for L3MBTL1, OCT-4, CG-β, and HAND1 mRNA expression. Statistical analysis was by 2-way ANOVA and Bonferroni posttest (*$P < 0.05$). Error bars represent the standard deviation ($n = 3$). **(B)** Phosphorylation of SMADS1/5/8 was examined by Western blot analysis in the homogenates of undifferentiated (day 1) and spontaneously differentiated (day 7) control LUC shRNA and L3MBTL1-KD cells. **(C)** Immunoassay for placental hormones CG-β and progesterone. Error bars represent the standard deviation ($n = 3$). **(D)** L3MBTL1 KD cells differentiate under defined conditions. Fluorescence images of typical neuronal rosette structures at day 9 of directed neuroectoderm differentiation for control LUC shRNA and L3MBTL1 KD cell lines (*upper panel*) are shown. Scale bar represents 50 μm. Representative images of 3 independent experiments are shown. Reverse transcriptase qPCR analysis results for neuroectoderm markers SOX-1 and PAX6 mRNA expression (*bottom panel*) are also shown. Statistical analysis was performed by 2-way ANOVA and Bonferroni posttest (*$P < 0.05$). Error bars represent the standard deviation ($n = 3$). Color images available online at www.liebertonline.com/scd

do express trophectoderm markers (Figs. 2E and 3B, D), and in fact, the increased expression of CDX2 is consistent with the L3MBTL1 KD cells being restricted to a trophoblast fate (Fig. 3A) [37]. Cdx2 acts early in the lineage hierarchy and its overexpression triggers embryonic stem cells to differentiate into trophoblast stem cells [26,27]. Overall, these changes could explain the failure of these cells to form typical EB structures in nonadherent assays. It is also possible that genomic instability during EB development could explain the increased cell death seen in L3MBTL1 KD cells (Fig. 2B, C), as we recently reported [20]. In contrast, the differentiated control cells maintained expression of embryonic lineage markers, and consistent with their upregulation of L3MBTL1, the expression of trophoblast markers was absent.

The production of extra-embryonic trophoblast cells from the L3MBTL1 KD cells resembles the effect of BMP4 on hESCs [22]. BMP4 directs hESCs toward trophoblast with increased SMAD 1/5/8 phosphorylation, CG-β secretion, and HAND1 expression, which occurs concomitantly with a marked decrease in L3MBTL1 expression (Fig. 4A, B). Both the BMP4-stimulated hESCs and the L3MBTL1 KD cells secrete placental hormones, demonstrating that knockdown of L3MBTL1 drives hESCs to become trophoblast-like cells (Fig. 4C). The lack of other embryonic cell types derived from L3MBTL1KD cells is not absolute, as L3MBTL1 KD cells can still form neural tissue and hematoendothelial cells in response to strong inductive signals. This suggests that L3MBTL1 may promote the retention of pluripotency of hESCs, at least in part by blocking trophoblast differentiation.

Thus, L3MBTL1 may play a role in the earliest cell fate decisions involved in human development, most likely by repressing genes involved in trophectoderm differentiation. Such a phenotype was recently described for Mbd3, a component of the Mi-2/NURD repressor complex [38]. L3MBTL1 may promote chromatin compaction via its recognition of mono- and dimethylated states of H4K20 by L3MBTL1 [17,18] or by recruiting additional chromatin remodelers to block the trophectoderm differentiation of hESCs. In *Drosophila*, dl(3)MBT has been shown to bind histone H4 K20 monomethyl in close association with the dRPD3 histone deacetylase, resulting in deacetylation of histone H4 K5/K12 [39]. However, we found that L3MBTL1 can repress gene expression in an HDAC-independent fashion [16]. L3MBTL1 could be a central component of a repressive complex that loses its function after L3MBTL1 KD. It is likely that multiple chromatin regulators control the differentiation process. For instance, the histone methyltransferase SETDB1 was recently shown to repress trophectoderm differentiation of mouse ESCs via H3K9 methylation [40]. The degree of histone H4K20 methylation is dynamically regulated during hESC differentiation. Mass spectrometry (MS) studies have revealed that a large percentage of histone H4 is dimethylated in undifferentiated hESCs (~65%) with some unmethylated (~20%) and some monomethylated (~10%) or trimethylated (~5%) residues. Following TPA treatment, unmethylated lysines are largely converted to dimethyllysines, and electron transfer dissociation-MS experiments have identified histone H4 K20 as the target of both methylation events [41]. Mice deficient for Suv4-20 h1/2, a H4K20 methyltransferase, display loss of di- and trimethyl H4K20 with consequent embryonic lethality [42]. ESCs have a poised epigenetic state that maintains chromatin in a structure ready for quick cell fate decisions [10]. The inner cell mass and trophectoderm possess different gene expression profiles. Consequently, their epigenetic profiles should also differ. We have not seen noticeable differences in the level of HP1γ, which binds L3MBTL1, or in H3K9 trimethylation, a heterochromatin mark recognized by HP1γ, between the spontaneously differentiated trophoblast cells and the induced neuroectoderm cells (Supplementary Fig. S3A). Nonetheless, epigenetic disturbance during the early events of differentiation may be a consequence of knocking down L3MBTL1, explaining the lineage selectivity of hESCs toward the trophectoderm fate.

In summary, L3MBTL1 KD hESCs proliferate normally in the undifferentiated state, but are impaired in their ability to spontaneously differentiate toward embryonic tissues, and preferentially differentiate into trophoblast tissue (Supplementary Fig. S3B). Further studies are required to establish the molecular basis of the lineage selectivity that occurs after L3MBTL1 knockdown.

Summary

To define how L3MBTL1, a chromatin-associated polycomb group protein with transcriptional repressive activities, regulates early events in embryonic cell differentiation, we created hESC lines that constitutively express shRNAs directed against L3MBTL1. Although the L3MBTL1 KD cells could be induced to differentiate into embryonic neuroectoderm, they adopted an exclusive trophoblast fate during spontaneous differentiation. The data suggest that L3MBTL1 depletion does not affect hESC self-renewal but impacts pluripotency; depletion of L3MBTL1 directs hESC differentiation toward extra-embryonic tissues, rather than embryo-derived tissues.

Acknowledgments

This work was supported by grants from The Starr Foundation and NIH (R01 grant CA102202 to S.D.N.) and by Lymphoma Research Foundation.

Author Disclosure Statement

The authors declare that no conflicts of interest exist.

References

1. Keller G. (2005). Embryonic stem cell differentiation: emergence of a new era in biology and medicine. Genes Dev 19:1129–1155.
2. Auman HJ, T Nottoli, O Lakiza, Q Winger, S Donaldson and T Williams. (2002). Transcription factor AP-2gamma is essential in the extra-embryonic lineages for early post-implantation development. Development 129:2733–2747.
3. Donnison M, A Beaton, HW Davey, R Broadhurst, P L'Huillier and PL Pfeffer. (2005). Loss of the extraembryonic ectoderm in Elf5 mutants leads to defects in embryonic patterning. Development 132:2299–2308.
4. Ralston A, BJ Cox, N Nishioka, H Sasaki, E Chea, P Rugg-Gunn, G Guo, P Robson, JS Draper and J Rossant. Gata3 regulates trophoblast development downstream of Tead4 and in parallel to Cdx2. Development 137:395–403.
5. Russ AP, S Wattler, WH Colledge, SA Aparicio, MB Carlton, JJ Pearce, SC Barton, MA Surani, K Ryan, MC Nehls, V Wilson and MJ Evans. (2000). Eomesodermin is required for

mouse trophoblast development and mesoderm formation. Nature 404:95–99.
6. Strumpf D, CA Mao, Y Yamanaka, A Ralston, K Chawengsaksophak, F Beck and J Rossant. (2005). Cdx2 is required for correct cell fate specification and differentiation of trophectoderm in the mouse blastocyst. Development 132:2093–2102.
7. Yagi R, MJ Kohn, I Karavanova, KJ Kaneko, D Vullhorst, ML DePamphilis and A Buonanno. (2007). Transcription factor TEAD4 specifies the trophectoderm lineage at the beginning of mammalian development. Development 134:3827–3836.
8. Yamamoto H, ML Flannery, S Kupriyanov, J Pearce, SR McKercher, GW Henkel, RA Maki, Z Werb and RG Oshima. (1998). Defective trophoblast function in mice with a targeted mutation of Ets2. Genes Dev 12:1315–1326.
9. Christophersen NS and K Helin. Epigenetic control of embryonic stem cell fate. J Exp Med 207:2287–2295.
10. Bernstein BE, TS Mikkelsen, X Xie, M Kamal, DJ Huebert, J Cuff, B Fry, A Meissner, M Wernig, K Plath, R Jaenisch, A Wagschal, R Feil, SL Schreiber and ES Lander. (2006). A bivalent chromatin structure marks key developmental genes in embryonic stem cells. Cell 125:315–326.
11. Peters AH, D O'Carroll, H Scherthan, K Mechtler, S Sauer, C Schofer, K Weipoltshammer, M Pagani, M Lachner, A Kohlmaier, S Opravil, M Doyle, M Sibilia and T Jenuwein. (2001). Loss of the Suv39h histone methyltransferases impairs mammalian heterochromatin and genome stability. Cell 107:323–337.
12. Pasini D, AP Bracken, MR Jensen, E Lazzerini Denchi and K Helin. (2004). Suz12 is essential for mouse development and for EZH2 histone methyltransferase activity. EMBO J 23:4061–4071.
13. Torres-Padilla ME, DE Parfitt, T Kouzarides and M Zernicka-Goetz. (2007). Histone arginine methylation regulates pluripotency in the early mouse embryo. Nature 445:214–218.
14. Wismar J, T Loffler, N Habtemichael, O Vef, M Geissen, R Zirwes, W Altmeyer, H Sass and E Gateff. (1995). The Drosophila melanogaster tumor suppressor gene lethal(3)-malignant brain tumor encodes a proline-rich protein with a novel zinc finger. Mech Dev 53:141–154.
15. Nimer SD. (2008). Myelodysplastic syndromes. Blood 111:4841–4851.
16. Boccuni P, D MacGrogan, JM Scandura and SD Nimer. (2003). The human L(3)MBT polycomb group protein is a transcriptional repressor and interacts physically and functionally with TEL (ETV6). J Biol Chem 278:15412–15420.
17. Trojer P, G Li, RJ Sims 3rd, A Vaquero, N Kalakonda, P Boccuni, D Lee, H Erdjument-Bromage, P Tempst, SD Nimer, YH Wang and D Reinberg. (2007). L3MBTL1, a histone-methylation-dependent chromatin lock. Cell 129:915–928.
18. Kalakonda N, W Fischle, P Boccuni, N Gurvich, R Hoya-Arias, X Zhao, Y Miyata, D Macgrogan, J Zhang, JK Sims, JC Rice and SD Nimer. (2008). Histone H4 lysine 20 monomethylation promotes transcriptional repression by L3MBTL1. Oncogene 27:4293–4304.
19. Perna F, N Gurvich, R Hoya-Arias, O Abdel-Wahab, RL Levine, T Asai, F Voza, S Menendez, L Wang, F Liu, X Zhao and SD Nimer. Depletion of L3MBTL1 promotes the erythroid differentiation of human hematopoietic progenitor cells: possible role in 20q- polycythemia vera. Blood 116:2812–2821.
20. Gurvich N, F Perna, A Farina, F Voza, S Menendez, J Hurwitz and SD Nimer. L3MBTL1 polycomb protein, a candidate tumor suppressor in del(20q12) myeloid disorders, is essential for genome stability. Proc Natl Acad Sci USA 107:22552–22557.
21. Ivanova N, R Dobrin, R Lu, I Kotenko, J Levorse, C DeCoste, X Schafer, Y Lun and IR Lemischka. (2006). Dissecting self-renewal in stem cells with RNA interference. Nature 442:533–538.
22. Xu RH, X Chen, DS Li, R Li, GC Addicks, C Glennon, TP Zwaka and JA Thomson. (2002). BMP4 initiates human embryonic stem cell differentiation to trophoblast. Nat Biotechnol 20:1261–1264.
23. Lee H, GA Shamy, Y Elkabetz, CM Schofield, NL Harrsion, G Panagiotakos, ND Socci, V Tabar and L Studer. (2007). Directed differentiation and transplantation of human embryonic stem cell-derived motoneurons. Stem Cells 25:1931–1939.
24. Sims JK and JC Rice. (2008). PR-Set7 establishes a repressive trans-tail histone code that regulates differentiation. Mol Cell Biol 28:4459–4468.
25. Beck F, T Erler, A Russell and R James. (1995). Expression of Cdx-2 in the mouse embryo and placenta: possible role in patterning of the extra-embryonic membranes. Dev Dyn 204:219–227.
26. Tolkunova E, F Cavaleri, S Eckardt, R Reinbold, LK Christenson, HR Scholer and A Tomilin. (2006). The caudal-related protein cdx2 promotes trophoblast differentiation of mouse embryonic stem cells. Stem Cells 24:139–144.
27. Niwa H, Y Toyooka, D Shimosato, D Strumpf, K Takahashi, R Yagi and J Rossant. (2005). Interaction between Oct3/4 and Cdx2 determines trophectoderm differentiation. Cell 123:917–929.
28. Riley P, L Anson-Cartwright and JC Cross. (1998). The Hand1 bHLH transcription factor is essential for placentation and cardiac morphogenesis. Nat Genet 18:271–275.
29. Hemberger M, M Hughes and JC Cross. (2004). Trophoblast stem cells differentiate *in vitro* into invasive trophoblast giant cells. Dev Biol 271:362–371.
30. Martindill DM, CA Risebro, N Smart, M Franco-Viseras Mdel, CO Rosario, CJ Swallow, JW Dennis and PR Riley. (2007). Nucleolar release of Hand1 acts as a molecular switch to determine cell fate. Nat Cell Biol 9: 1131–1141.
31. Scott IC, L Anson-Cartwright, P Riley, D Reda and JC Cross. (2000). The HAND1 basic helix-loop-helix transcription factor regulates trophoblast differentiation via multiple mechanisms. Mol Cell Biol 20:530–541.
32. Jaquemar D, S Kupriyanov, M Wankell, J Avis, K Benirschke, H Baribault and RG Oshima. (2003). Keratin 8 protection of placental barrier function. J Cell Biol 161:749–756.
33. Simmons DG and JC Cross. (2005). Determinants of trophoblast lineage and cell subtype specification in the mouse placenta. Dev Biol 284:12–24.
34. Mi S, X Lee, X Li, GM Veldman, H Finnerty, L Racie, E LaVallie, XY Tang, P Edouard, S Howes, JC Keith, Jr. and JM McCoy. (2000). Syncytin is a captive retroviral envelope protein involved in human placental morphogenesis. Nature 403:785–789.
35. Vodyanik MA and II Slukvin. (2007). Hematoendothelial differentiation of human embryonic stem cells. Curr Protoc Cell Biol Chapter 23:Unit 23.6.
36. Meshorer E and T Misteli. (2006). Chromatin in pluripotent embryonic stem cells and differentiation. Nat Rev Mol Cell Biol 7:540–546.

37. Jedrusik A, DE Parfitt, G Guo, M Skamagki, JB Grabarek, MH Johnson, P Robson and M Zernicka-Goetz. (2008). Role of Cdx2 and cell polarity in cell allocation and specification of trophectoderm and inner cell mass in the mouse embryo. Genes Dev 22:2692–2706.
38. Zhu D, J Fang, Y Li and J Zhang. (2009). Mbd3, a component of NuRD/Mi-2 complex, helps maintain pluripotency of mouse embryonic stem cells by repressing trophectoderm differentiation. PLoS One 4:e7684.
39. Scharf AN, K Meier, V Seitz, E Kremmer, A Brehm and A Imhof. (2009). Monomethylation of lysine 20 on histone H4 facilitates chromatin maturation. Mol Cell Biol 29:57–67.
40. Lohmann F, J Loureiro, H Su, Q Fang, H Lei, T Lewis, Y Yang, M Labow, E Li, T Chen and S Kadam. (2009). KMT1E mediated H3K9 methylation is required for the maintenance of embryonic stem cells by repressing trophectoderm differentiation. Stem Cells 28:201–212.
41. Phanstiel D, J Brumbaugh, WT Berggren, K Conard, X Feng, ME Levenstein, GC McAlister, JA Thomson and JJ Coon. (2008). Mass spectrometry identifies and quantifies 74 unique histone H4 isoforms in differentiating human embryonic stem cells. Proc Natl Acad Sci USA 105:4093–4098.
42. Schotta G, R Sengupta, S Kubicek, S Malin, M Kauer, E Callen, A Celeste, M Pagani, S Opravil, IA De La Rosa-Velazquez, A Espejo, MT Bedford, A Nussenzweig, M Busslinger and T Jenuwein. (2008). A chromatin-wide transition to H4K20 monomethylation impairs genome integrity and programmed DNA rearrangements in the mouse. Genes Dev 22:2048–2061.

Address correspondence to:
Dr. Stephen D. Nimer
Molecular Pharmacology and Chemistry Program
Sloan-Kettering Institute
Memorial Sloan-Kettering Cancer Center
1275 York Avenue, Box 575
New York, NY 10065

E-mail: nimers@mskcc.org

Received for publication September 29, 2010
Accepted after revision February 22, 2011
Prepublished on Liebert Instant Online February 22, 2011